Epitaxial interfaces between half-crystals of quasicrystalline and periodic material

Epitaxial interfaces between half-crystals of quasicrystalline and periodic material

W Theis[1] and K J Franke[2]

[1] Nanoscale Physics Research Laboratory, School of Physics and Astronomy, University of Birmingham, Birmingham B15 2TT, UK
[2] Institut für Experimentalphysik, Freie Universität Berlin, Arnimallee 14, 14195 Berlin, Germany

E-mail: w.theis@bham.ac.uk

Abstract
We recently demonstrated that epitaxial interfaces can be formed between periodic and quasiperiodic materials (Franke *et al* 2007 *Phys. Rev. Lett.* **99** 036103). Such interfaces exhibit the same defining characteristic as epitaxial interfaces between commensurate periodic materials, namely the *locking into registry* of the two half-crystals' atomic structures. This real space characteristic is equivalent to the requirement of a coincidence of reciprocal lattice points. Here, we explore the characteristics of the potential interfaces within the class of quasicrystals exhibiting a periodic direction, including decagonal quasicrystals. We derive our results geometrically from a higher dimensional description, thus providing visual insight into the underlying concepts. Since the reciprocal lattice of quasicrystalline structures is generated by more basis vectors than their periodic counterparts', suitable quasicrystalline interlayers can be designed to epitaxially link incommensurate half-crystals. We give examples of selected model structures as illustrations.

(Some figures in this article are in colour only in the electronic version)

1. Introduction

Modern device technology relies on building well-defined structures from a range of different materials. Typically, the best control and device performance is achieved when the involved interfaces are epitaxial, yielding a perfect registry at the atomic level. This provides an optimal homogeneity along the interface, thus avoiding dislocations or other structural or electronic defects which would be detrimental to the device's performance. In the case of periodic crystals, a registry at the atomic level is achieved when the two half-crystals share a common interface unit cell, which defines an epitaxial (commensurate) interface in thin films.

Because quasicrystals, lacking periodicity, have no unit cell one might have thought this precludes epitaxy between quasicrystals and periodic materials. However, as we showed recently [1] it does not, as the essence of epitaxy is not the common unit cell but a *locking into registry* at the interface. The latter describes the fact that the energy of a commensurate interface has local minima with regard to lateral shifts of one of the half-crystals with respect to the other [2]. Taking

this as a starting point, we were able to demonstrate that for interfaces of any combination of periodic or quasiperiodic crystals, epitaxy is characterized by the half-crystals having at least two non-collinear interface projected reciprocal lattice vectors in common. As quasicrystals have an higher number of reciprocal lattice basis vectors, this has the fascinating consequence that quasicrystalline interlayers can epitaxially link incommensurate materials.

In the following subsections we will briefly review the first experimental realization of an epitaxial interface between a periodic and quasiperiodic material and the underlying concepts [1]. In this epitaxial system, the decagonal Al–Ni–Co quasicrystal forms an interface plane with an orientation neither parallel nor perpendicular to its periodic axis. We will explore the nature of such tilted orientations in quasicrystals including a periodic direction with regard to epitaxy by utilizing a higher dimensional visual approach.

1.1. Experimental realization: AlAs/Al–Ni–Co

There is a wide range of studies involving film or monolayer growth on quasicrystal surfaces. A number of these have
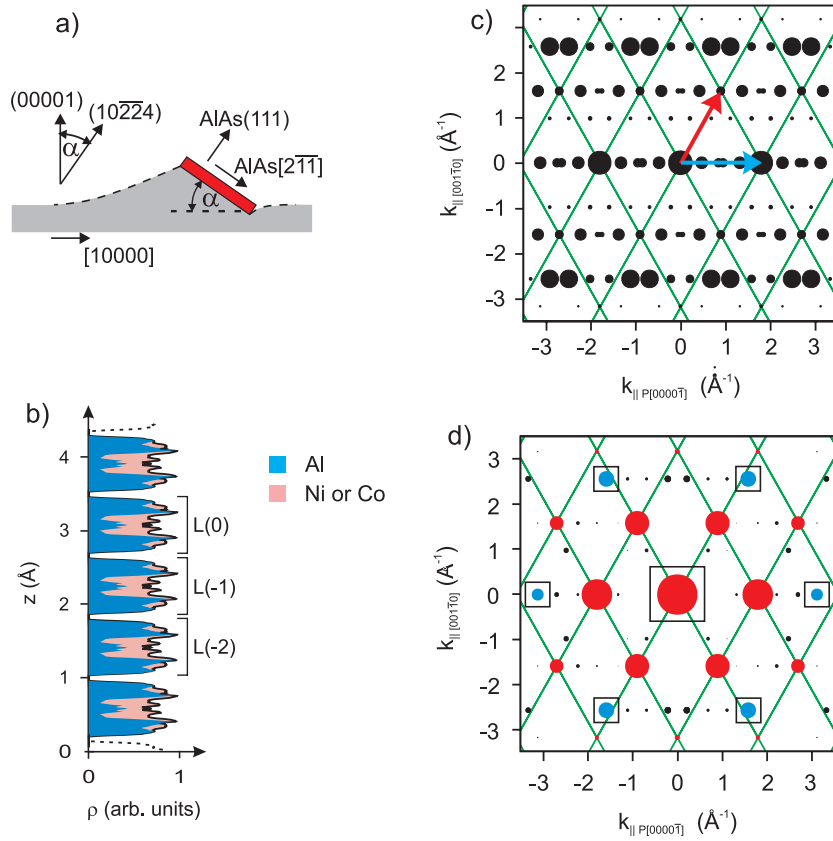
Figure 1. Epitaxial interface between strained AlAs(111) and Al–Ni–Co(10$\bar{2}\bar{2}$4). (a) Interface geometry with faceted substrate (light gray, $\alpha = 35.15°$) and the in-plane orientation of the strained AlAs(111)-film. (b) Al–Ni–Co(10$\bar{2}\bar{2}$4) areal atomic density $\rho(z)$ in the planes perpendicular to the [10$\bar{2}\bar{2}$4] direction. (c) Al–Ni–Co reciprocal lattice projected onto the (10$\bar{2}\bar{2}$4) interface plane (black circles) and strained AlAs(111) film reciprocal lattice points (vertices of the mesh). (d) Fourier transform of the top layer of bulk truncated Al–Ni–Co(10$\bar{2}\bar{2}$4), marked as L(0) in (b). A strong set for potential alternate epitaxy is outlined by squares. The radii of the circles in (c) and (d) are proportional to the Fourier amplitudes of the atomic density of Al–Ni–Co bulk and single layer L(0), respectively, calculated from the structural model by Yamamoto and Weber [3].

reported interfaces with a defined relative orientation between a periodic layer and a quasicrystalline substrate [4–9]. The orientational alignment in these systems, however, does not originate from the formation of an epitaxial interface as defined above. Instead, in these cases it is due to either local matching of clusters, local symmetry at preferred nucleation sites, or long length-scale strain modulations localized at the interface. The orientational alignment described by Widjaja and Marks [9, 10] is particularly noteworthy as it results from an interface energy minimization for an extended (infinite) interface plane. It corresponds to the case of an interface between periodic systems with slightly differing lattice constants, which in first order provides a modulation of the atomic positions at the interface, and at higher order can generate a dislocation network. These atomic shifts provide energy minima with respect to rotations of the half-crystals with respect to each other, yet they do not yield energy minima with regard to lateral shifts between the half-crystals which are a characteristic of commensurate epitaxial interfaces.

Recently, however, we have been able to observe full fledged epitaxy between periodic and quasiperiodic half-crystals. In the experiment discussed in detail in [1], exposing the ten fold surface of decagonal Al$_{71.8}$Ni$_{14.8}$Co$_{13.4}$

to a molecular beam of As was shown to lead to the formation of Al–Ni–Co(10$\bar{2}\bar{2}$4) facets overgrown by strained AlAs(111) films. The observed interface geometry is depicted in figure 1(a). The epitaxial nature of the interface was demonstrated by projecting the known bulk reciprocal lattice structure of Al–Ni–Co onto the (10$\bar{2}\bar{2}$4) interface plane (solid black circles in figure 1(b)) and comparing this to the experimentally determined AlAs(111) reciprocal lattice structure (vertices of green grid in same figure). The two half-crystals share the two non-collinear interface projected reciprocal lattice vectors indicated in the figure, thus fulfilling the criterion for epitaxy.

The fact that the AlAs(111) film is strained by a few percent points towards a strong driving force to retain the atomic registry at the interface. To understand its origin we considered a simple model for the interface binding energy E in which interface atoms interact by a pair potential $V(\mathbf{r})$ with $\mathbf{r}$ the lateral displacement. This yields [1]

$$E(\mathbf{r}_s) \propto \int \int \rho_1(\mathbf{r}_1 - \mathbf{r}_s)\rho_2(\mathbf{r}_2) V(\mathbf{r}_1 - \mathbf{r}_2) \, \mathrm{d}^2 r_1 \, \mathrm{d}^2 r_2$$
$$\propto \sum_{\mathbf{G}} \hat{\rho}_1(-\mathbf{G})\hat{\rho}_2(\mathbf{G})\hat{V}(\mathbf{G})e^{-i\mathbf{G}\mathbf{r}_s}$$
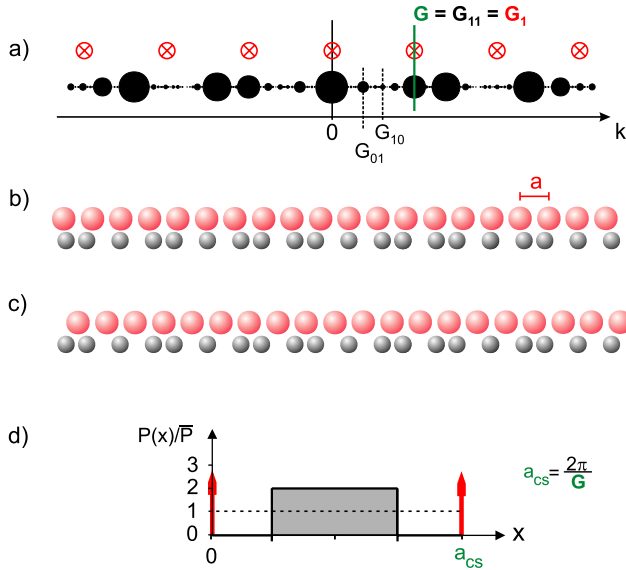
Figure 2. Epitaxial interfaces between a periodic and a Fibonacci chain. (a) Reciprocal lattices. The radii of the black circles are proportional to the magnitude of the corresponding Fourier components of the Fibonacci chain. The common reciprocal lattice vector is $G = G_{11}^{\mathrm{Fib}} = G_1 = 2\pi/a$. (b) Real space structure for an attractive interaction (favoring on-top sites). (c) Real space structure for a relative shift of $a/2$ with respect to (b). (d) Average distribution of the Fibonacci chain atoms within the unit cell of the periodic chain.

with $\mathbf{r}_S$ the lateral shift of the half-crystals with respect to each other, $\rho_{1,2}$ the atomic densities of the two interface layers, $\hat{\rho}_{1,2}$ and $\hat{V}$ the respective Fourier transforms, and $\mathbf{G}$ the common reciprocal lattice vectors. This illustrates that the locking into registry can only be strong if both half-crystal's structure factors $\hat{\rho}_{1,2}(\mathbf{G})$ are large for at least one of the common reciprocal lattice vector $\mathbf{G} \neq 0$.

Calculating these structure factors for our experimental system required identifying a top layer at the interface. As was reported [1] and will be discussed in detail for a model system in the next section, the areal atomic density in a decagonal quasicrystal along a tilted crystallographic orientation is periodic. For Al–Ni–Co($10\bar{2}\bar{2}4$) this density drops to zero periodically thus defining individual layers (figure 1(c)). Taking the Fourier transform of an individual layer reveals large structure factors predominantly for those vectors common to the AlAs(111) interface structure. In order to understand how this is linked to the real space atomic structure we briefly review some results for the very simplest mixed epitaxial system, namely that between a periodic and a Fibonacci chain.

1.2. Locking into registry

The real space implications of a *locking into registry* of an epitaxial interface between periodic and quasiperiodic systems is best illustrated by considering the interface between a Fibonacci and a periodic chain. A Fibonacci chain (figure 2(b), lower row) consists of atoms arranged quasiperiodically along a line with nearest-neighbor distances L and S with $L = \tau S$ and $\tau = (1+\sqrt{5})/2$ the golden mean. The distance L occurs τ times as often as S, thus yielding an average distance between atoms of $\bar{a} = (\tau L + S)/(\tau + 1) = S(3 - \tau)$. (A detailed construction of a Fibonacci chain is presented in section 2.1 below.)

The diffraction pattern of the Fibonacci chain (figure 2(a), solid circles) is generated by two incommensurate vectors G_{10} and $G_{01} = G_{10}/\tau$. Choosing the basis vector G_1 of the reciprocal lattice of the periodic chain to match G_{11}, we arrive at the epitaxial interface shown in figure 2. This particular choice is unique in that the lattice constant a of the atomic chain is identical to the mean atomic distance $\bar{a}$ of the
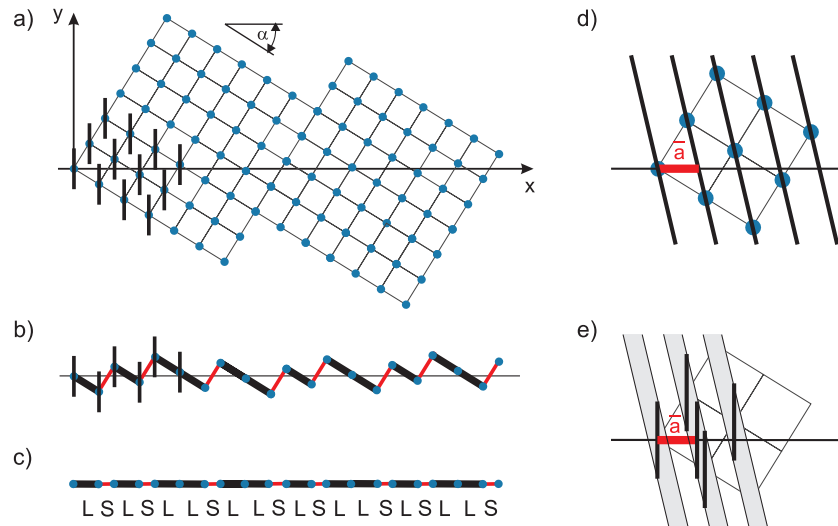

Figure 3. Higher dimensional construction of the Fibonacci chain and its average distribution of atoms within a periodic unit cell. (a) Two-dimensional square lattice with atomic surfaces (vertical lines attached to vertices of the grid) and physical space x-coordinate and perpendicular space y-coordinate. (b) The subset of vertices whose atomic surfaces cut the real space x-axis and the connecting edges. (c) Projection of structure in (b) onto the x-axis, yielding the Fibonacci chain with its quasiperiodic sequence of long (L) and short (S) segments. (d) Relation of the average distance $\bar{a}$ between Fibonacci atoms to the 2d square lattice. (e) Construction of the average distribution of Fibonacci atoms in the periodic unit cell. See the main text for details.
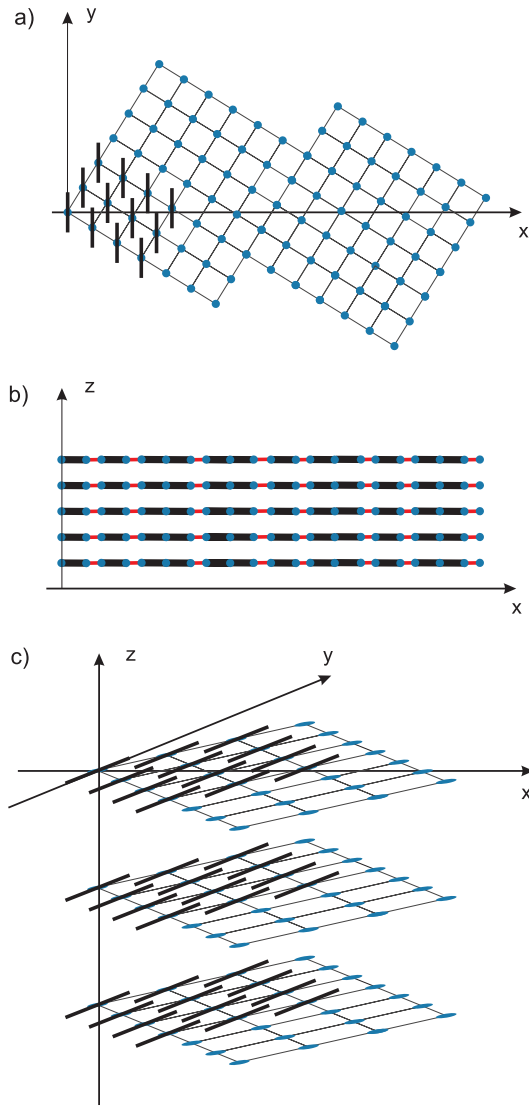
Figure 4. Higher dimensional construction of a periodic stacking of
Fibonacci chains. (a) Square lattice with atomic surfaces and
physical space x-coordinate and non-physical space y-coordinate.
(b) Periodic stacking along the z-axis showing projections of
segments corresponding to those in figure 3(c). (c) View of the 3d
higher space structure. The atomic surfaces are line segments parallel
to the non-physical space y-direction.

Fibonacci chain. The *locking into registry* is illustrated by the
two different lateral shifts of the chains depicted in figures 2(b)
and (c). In (b) a preference for on-top alignment is apparent,
while in (c) bridge sites are favored. The distribution of the
Fibonacci atoms within the unit cell of the periodic chain $P(x)$
is shown in panel (d) for alignment (c). Since this distribution
is not uniform a lateral shift of the chains with respect to each
other will modify the interface energy and thus provide the
energetic minima and the *locking into registry* of the interface
structure.

2. Description from higher dimension

The structural properties relevant for epitaxy, such as the
areal density $\rho(z)$ depicted in figure 1 and the probability

distribution $P(\vec{r})$ of a quasicrystal's atoms in an epitaxial
periodic unit cell can be easily calculated numerically from the
quasicrystal's bulk atomic structure. However, to gain insight
into their origin it is helpful to derive these geometrically for
a representative model structure. This can be done by utilizing
the well established construction of quasicrystals from higher
dimensional periodic structures [11–14].

2.1. One-dimensional structure

We start out with a periodic square lattice with lattice constant
a tilted by an angle α with $\tan(\alpha) = 1/\tau$ with respect to
an x-axis (figure 3(a)). The x- and y-direction are called
physical and non-physical direction, respectively. In the next
step, atomic surfaces are attached to the vertices of the square
lattice. These atomic surfaces are line segments of length
$\Delta = a(\cos(\alpha) + \sin(\alpha))$ which are aligned perpendicular to
the physical space x-direction. The periodic structure is then
cut along the physical space x-direction and the intersections
with the atomic planes yield the atomic sites. By retaining the
edges of the square lattice which link atomic surfaces cutting
the physical plane the generation of the L and S segments from
the two basis vectors of the square lattice becomes apparent
(figures 3(b) and (c)).

This higher dimensional construction of the Fibonacci
chain allows us to understand the origin of the non-uniformity
of the distribution of its atoms in the epitaxial unit cell as
depicted in figure 2 above. For the epitaxial match with
$G_1 = G_{11}$, the lattice constant of the periodic chain is equal to
the mean distance $\bar{a}$ and given by the intersection of the x-axis
with the square lattice's (11)-netplanes as shown in figure 3(d).

In order to derive the average distribution in the unit cell,
we translate the Fibonacci chain by every integer multiple
of $\bar{a}$ and record all atoms falling into a single selected unit
cell. Translating the square lattice by $\bar{a}$ shifts its vertices
from one (11)-netplane to the next. As the vertex at the
origin is the only vertex in the original square lattice which
is on the x-axis (otherwise the structure would be periodic),
translating the lattice by arbitrary integer multiples of $\bar{a}$ will
never yield a vertex shifted exactly onto another. Thus, the
netplanes are covered homogeneously by the shifted vertices.
The atomic surfaces attached to the vertices generate uniform
stripes centered on the netplanes as shown in figure 3(e).
Moving along the physical space x-axis, regions within the
stripe have a uniform probability of finding Fibonacci chain
atoms in the corresponding part of the periodic chain's unit
cell, while regions between stripes yield a zero probability.
The method of calculating the probability $P(x)$ used here
mirrors that introduced by Steurer and Haibach [15] for the
determination of the periodic average structure.

2.2. Tilted orientation of stacked Fibonacci chains

The experimental system in which we observed epitaxy
featured a decagonal quasicrystal, which is characterized by
a periodic stacking of quasicrystalline planes. The interface
plane was tilted with respect to these. To capture these essential
features in a model system we explore a periodic stacking of
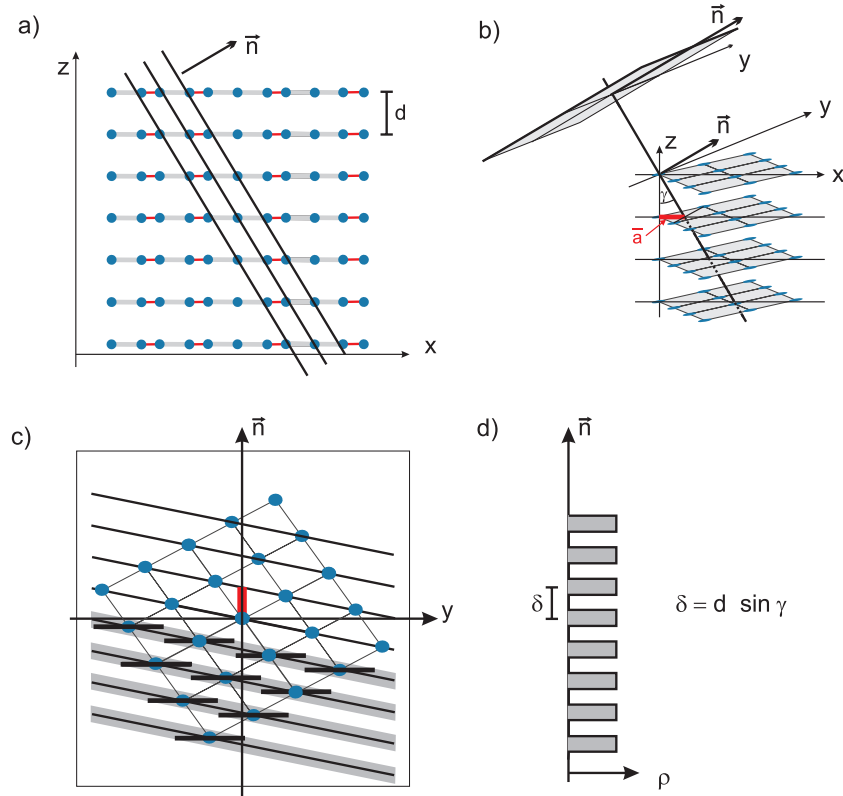Fibonacci chains (figure 4). As above, the Fibonacci chains

Figure 5. Derivation of the atomic areal density distribution along a tilted orientation. (a) Atomic physical space structure and broadened netplanes for an orientation given by the vector $\vec{n}$. (b) Surface normal $\vec{n}$ shown in a 3d view of the periodic higher dimensional structure with y the non-physical axis. The angle γ between x-axis and $\vec{n}$ (and between z-axis and netplanes) is given by $\tan \gamma = \bar{a}/d$. (c) Projection of a single x, y-plane onto the $\vec{n}, y$-plane. The gray bands reflect the area into which projections of all atomic surfaces including those with $z \neq 0$ fall. (d) Resulting areal density along the surface normal $\vec{n}$ with periodicity of $\delta = d \sin \gamma$.

run along the x-direction. They are stacked with periodicity d along a perpendicular z-direction. The higher dimensional periodic structure describing this is a periodic stacking of a square lattice with corresponding atomic surfaces (figure 4(c)). The non-physical direction is again the y-direction and the physical space structure is generated by a cut along the x, z-plane.

We now consider a tilted crystallographic orientation of this two-dimensional quasicrystal, choosing an angle γ between surface normal $\vec{n}$ and z-direction to give $\tan(\gamma) = \bar{a}/d$ as illustrated in figure 5(b). This corresponds to a (111) orientation. Our first interest is to calculate the x-integrated atomic density along the surface normal $\vec{n}$. For this, we initially project the periodic 3d structure onto the $\vec{n}, y$-plane indicated in figure 5(b). A single square lattice corresponding to a single Fibonacci chain yields the projection in figure 5(c). Projecting all other square lattices onto the same $\vec{n}, y$-plane projects all vertices onto the projected (11)-netplanes in a similar fashion as discussed in regard to figure 3. This is the case because the intersection of the x-axis with each of the square lattices coincides with one of its respective (11)-netplanes. The first intersection is at the origin, the next is through the first (11)-netplane by definition of the angle γ, all others intersect at netplanes because both z-stacking and netplane stacking are periodic. The shifts of the vertices along the netplanes are incommensurate to the distance between vertices along a

netplane of an individual square lattice. Thus, projecting all atomic surfaces generates the stripes shown in figure 5(c). The final step to arrive at the density is to cut the projected structure along $y = 0$. This yields the periodicity and box-like shape of the x-integrated density shown in figure 5(d). The periodicity is $\delta = d \sin(\gamma)$.

Having identified the individual broadened layers in our model structure, we come to the question of the distribution of the atoms within one of these layers, which determines the interface structure and energy. Because the empty space between layers is as extended as the layers themselves, we can pick any atom and define its layer as those atoms within a band of $\pm \delta/2$ with respect to the surface normal direction $\vec{n}$. As can be seen in figure 6(b), in our simple case, the lateral distance between neighboring atoms in a given layer takes one of two values L_{11} or S_{11} generated by a combination of stepping along the Fibonacci chain by L or S, respectively, and stepping a distance d onto the next chain. The sequence within the layer is again a Fibonacci sequence, the L_{11} and S_{11} segment lengths, however, are no longer related by the factor τ.

While we have characterized the sequence explicitly in this simple case, for epitaxy the critical information is the distribution of the quasicrystalline layer's atoms within the periodic unit cell of the counterpart of the interface. This can be derived geometrically. First, consider the real space atomic structure of figure 6(a). From this we want to generate the
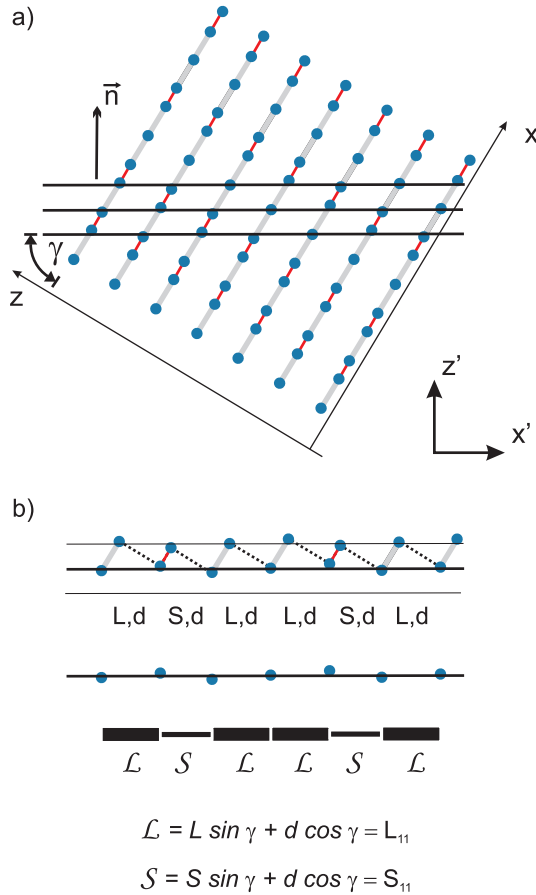
Figure 6. Atomic sites in the surface layer of a tilted orientation.
(a) Tilted atomic configuration for $\vec{n}$ parallel to G_{111} as in figure 5.
(b) Construction of a single broadened netplane, see the text for
details.

lateral distribution of the atoms of a single layer. This can
be achieved by attaching atomic surfaces (segments of length
δ, parallel to $\vec{n}$, the z'-direction) to all atoms as shown in
figure 7(a). A cut along one of the horizontal lines would
then yield the lateral distribution of atoms in a single layer
by projecting the atoms of a single layer onto the line. In
order to be able to determine the distribution of these projected
atomic sites this procedure has to be performed based on the
3d periodic higher dimensional structure. Thus, the atomic
surface attached to every vertex of the square lattices will now
in fact be a 2d surface extending by Δ along the non-physical
y-direction and by δ along the z'-direction (see figures 7(b)
and (c)). The three required steps are: translations by the
periodic unit cell size along x', cut along $y = 0$, and cut
along $z' = 0$. The periodic unit cell size depends on the
epitaxial interface match selected. Here we chose again an
interface with an average of one quasicrystalline atom per
unit cell. This yields the unit cell size $\bar{b} = d/\cos(\gamma)$ as
depicted in figure 7(b). Translation by $\bar{b}$ along x' corresponds
to translating by $\bar{a}$ along x and by one unit cell along z,
such that the translations yield an x, y-plane (figure 7(d)) with
identical stripes as in the single Fibonacci chain (figure 3(e)).
In the present case, however, the 2d atomic surfaces extend
along the z'-direction. This results in the x, z-plane depicted
in figure 7(e). Finally this is cut along the x'-axis yielding the

probability $P(x')$ to find an atom of the tilted layer at location
x' within the periodic unit cell (figure 7(f)). It is particularly
noteworthy that the lateral distribution of the layer's atoms
within the periodic unit cell is significantly more localized than
in the case of the Fibonacci chain itself.

3. Quasicrystalline interlayers

Having gained a detailed understanding of the epitaxial inter-
face properties of quasicrystals including periodic directions,
we now consider the implications for quasicrystalline interlay-
ers linking half-crystals of periodic materials. Discussing epi-
taxy, the first question must be in regard to the interface pro-
jected reciprocal lattice vectors.

We again take periodically stacked Fibonacci chains as an
example. Its reciprocal lattice is spanned by a vector G_p along
the periodic direction and the two τ-scaled vectors G_{10} and
G_{01} pointing along the chains. When projecting the latter two
onto the interface plane their τ-scaling is retained as both are
shortened by the same factor. Since the interface is required to
have a crystallographic orientation (and we do not consider the
trivial case of the interface normal perpendicular to the periodic
direction), the projection of G_p is a linear combination of the
other two and can therefore be ignored. Thus, independent
of the selected interface orientation, the interface projected
reciprocal lattice structure is generated by two basis vectors
related by τ and we can confine our discussion to the interface
normal parallel to the periodic direction as shown in figure 8.
Similarly, if we consider a decagonal quasicrystal, tilting the
interface orientation along a high symmetry axis does not
provide new ratios between reciprocal lattice vectors along that
direction.

While the tilt orientation does not impact on the relative
lengths of the interface projected reciprocal lattice vectors, it
does, of course, have a strong impact on the atomic structure
of the interface layer. In figure 6 we saw, for example, that
the ratio of the observed nearest-neighbor distances can change
from τ to smaller values. The range of possible ratios also
includes commensurate values (rational numbers). Figure 9
illustrates an example of a Fibonacci sequence of nearest-
neighbor distances L and S with $L = 2S$. This provides an
interface with interface atoms of the quasicrystalline interlayer
perfectly aligned in the bridge sites of a periodic structure with
interface lattice constant of S (top interface in figure).

Linking half-crystals with interface lattice vectors
not scaling with τ, on the other hand, would require
quasicrystalline structures beyond those based on Fibonacci
sequences. However, it is always possible to construct a
suitable model quasicrystalline structure. Were we interested
in linking (100) and (110) half-crystals of the same simple
cubic material, for example, then we would need to generate
a quasicrystalline structure with a $\sqrt{2}$ scaling of its in-plane
reciprocal lattice vectors such as the one shown in figure 10.

We have seen that epitaxy provides a registry at the
interface. In periodic materials this registry extends across
interlayers such that in an epitaxial ABC system there is
also a registry between A and C. Thus, if AB and BC are
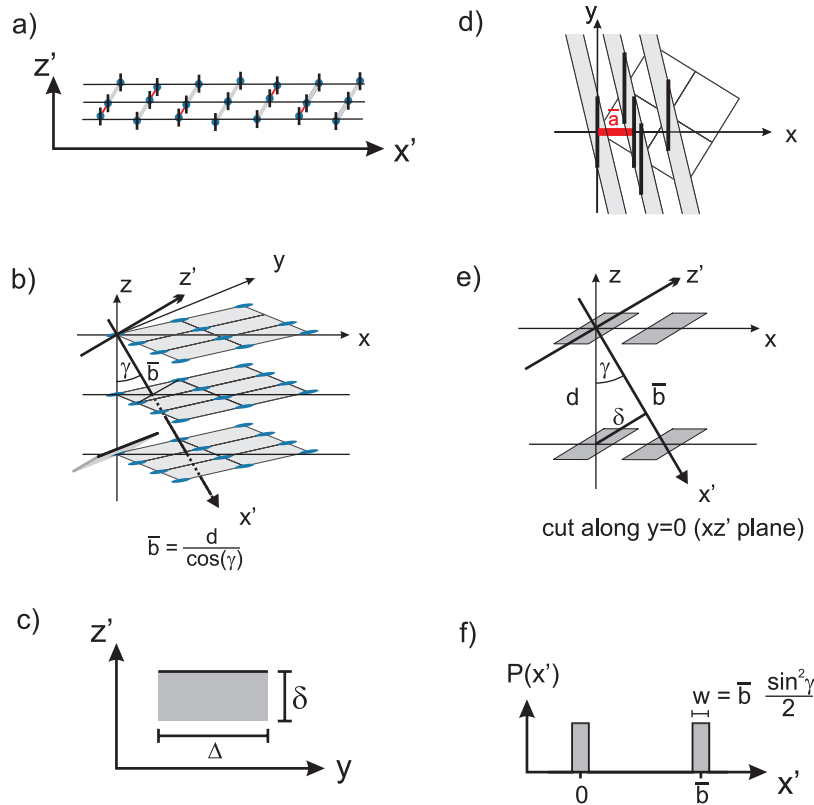epitaxial interfaces, so is AC. In systems with a quasicrystalline

Figure 7. Average distribution of surface layer atoms in a commensurate periodic unit cell. (a) Broadened netplanes with atomic surfaces generating a projection of the atoms onto their corresponding netplane. (b) Higher dimensional structure in 3d view with 2d atomic surface attached, only one of which is shown for clarity. $\bar{b}$ is the size of the unit cell of the commensurate structure. (c) Rectangular atomic surface with length Δ along the y-direction, generating the Fibonacci sequences, and height δ along the z-direction, generating the projection onto a single netplane. (d) Cut along an x, y-plane. Black vertical lines are the intersections with the 2d atomic surfaces, the gray bands the areas onto which these fall when shifting by $\bar{a}$ along x, which corresponds to the shift of $\bar{b}$ along the interface. (e) Cut along the x, z-plane (not a 3d view!) with the gray parallelograms resulting from the $y = 0$ cut through the stripes of (d) and extended along z to a length of δ in accordance with (c). (f) Resulting distribution in the unit cell of size $\bar{b}$ by cutting (e) along the x'-axis.
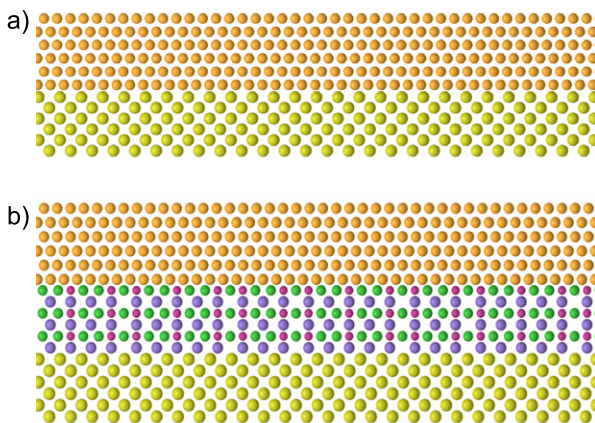

Figure 8. Quasicrystalline interlayer epitaxially linking incommensurate materials. (a) Direct non-epitaxial interface between the two incommensurate materials. The nearest-neighbor distances in the interface top layers scale as $1:\tau$. (b) Same half-crystals with a quasicrystalline interlayer which provides an epitaxial match to both simultaneously.

Figure 9. Quasicrystalline interlayer with $L = 2S$ providing an exact matching of the interlayer's atoms to the bridge sites of the top half-crystal.

interface linking incommensurate half-crystals this is clearly not the case. This implies that similar to the direct incommensurate interface (figure 8(a)) any arbitrary relative
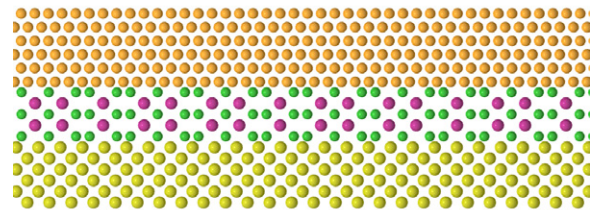
shift of the half-crystals can provide the same minimum energy when linked by the epitaxial interlayer. There is, however, a crucial difference. Without an interlayer, the half-crystals can slide along each other without having to overcome an energetic barrier. With the interlayer in place, this is no longer possible. When shifting the top half-crystal by small distances the interlayer has to be shifted by arbitrarily large distances in order to retaining a minimum energy configuration of the interfaces. Shifting the interlayer with respect to both half-crystals, on the other hand, requires overcoming the energy barriers resulting from the expitaxial match at these interfaces.
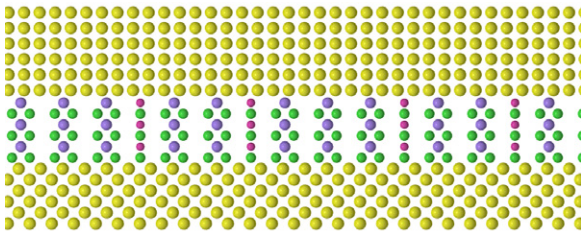
Figure 10. Quasicrystalline interlayer epitaxially linking (100) and (110) half-crystals of a simple cubic material.

To illustrate this, we consider a system resembling figure 8 with interface lattice constants a and τa of the top and bottom half-crystals, respectively, and $2\pi/a$ and $2\pi/(\tau a)$ the corresponding common interface projected reciprocal lattice vectors. Then the minimum energy configuration with the top half-crystal shifted by ϵa would require a shift of the interlayer by $m\tau a$ such that $\epsilon a = m\tau a - na$, with m, n integers in order to achieve the minimum energy registry at the respective interfaces. Small changes in ϵ require arbitrarily large changes in n, m to retain $\epsilon = m\tau - n$. To achieve a minimum energy configuration at a shift of $\epsilon < 0.1$, for example, the interlayer would have to be shifted by a distance of 5, 8, or more lattice constants τa, where 5, 8, ... are Fibonacci numbers.

4. Conclusions

The study of epitaxy between periodic and quasiperiodic materials provides fundamental insight into the nature of epitaxial interfaces. It illustrates that epitaxy is governed by a coincidence of reciprocal lattice points and that the existence of a common unit cell in epitaxial interfaces of periodic materials is simply a consequence of their periodicity and not the primary characteristic of epitaxy. An understanding of epitaxy between quasiperiodic and periodic materials opens the fascinating possibility of epitaxially linking incommensurate materials through quasicrystalline interlayers.

Exploring a model system of stacked Fibonacci chains we gained insight into epitaxy of decagonal and other quasicrystals featuring a periodic direction. The periodic axis generates a periodic netplane structure perpendicular to mixed crystallographic interface orientations as illustrated geometrically in a higher dimensional description. The non-uniformity of the lateral distribution of the interface atoms within the unit cell of the periodic interface side reflects the epitaxial match and the energy gained by the atomic *locking into registry* at the interface. For our chosen (111) orientation this distribution was found to be significantly more localized than for the non-tilted orientation. This hints at an energetic preference towards interfaces with tilted orientation, such as the one observed experimentally in strained AlAs(111) on Al–Ni–Co($10\bar{2}\bar{2}4$).

References

[1] Franke K J, Gille P, Rieder K-H and Theis W 2007 Achieving epitaxy between incommensurate materials by quasicrystalline interlayers *Phys. Rev. Lett.* **99** 036103
[2] Zangwill A 1990 *Physics at Surfaces* (Cambridge: Cambridge University Press)
[3] Yamamoto A and Weber S 1997 Five-dimensional superstructure model of decagonal Al–Ni–Co quasicrystals *Phys. Rev. Lett.* **78** 4430
[4] Shen Z, Kramer M J, Jenks C J, Goldman A I, Lograsso T, Delaney D, Heinzig M, Raberg W and Thiel P A 1998 Crystalline surface structures induced by ion sputtering of Al-rich icosahedral quasicrystals *Phys. Rev.* B **58** 9961–71
[5] Bolliger B, Erbudak M, Vvedensky D D, Zurkirch M and Kortan A R 1998 Surface structural transitions on the icosahedral quasicrystal Al$_{70}$Pd$_{20}$Mn$_{10}$ *Phys. Rev. Lett.* **80** 5369–72
[6] Shimoda M, Sato T J, Tsai A P and Guo J Q 2000 Epitaxial crystalline film with psuedo-tenfold symmetry formed by Au-deposition on a decagonal Al$_{72}$Ni$_{12}$Co$_{16}$ quasicrystal *Phys. Rev.* B **62** 11288–91
[7] Bolliger B, Dmitrienko V E, Erbudak M, Lüscher R, Nissen H-U and Kortan A R 2001 Epitactic textures of fcc Al on icosahedral Al–Pd–Mn quasicrystal *Phys. Rev.* B **63** 052203
[8] Fournée V, Cai T C, Ross A R, Lograsso T A, Evans J W and Thiel P A 2003 Nucleation and growth of Ag films on a quasicrystalline AlPdMn surface *Phys. Rev.* B **67** 033406
[9] Widjaja E J and Marks L D 2003 Epitaxial decagonal thin films on crystalline substrates *Phil. Mag. Lett.* **83** 47
[10] Widjaja E J and Marks L D 2003 Coincidence of reciprocal lattice planes model for quasicrystal–crystal epitaxy *Phys. Rev.* B **68** 134211
[11] Bak P 1985 Phenomenological theory of icosahedral incommensurate ('quasiperiodic') order in Mn–Al alloys *Phys. Rev. Lett.* **54** 1517–9
[12] Janssen T 1986 Crystallography of quasi-crystals *Acta Crystallogr.* A **42** 261–71
[13] Yamamoto A 1996 Crystallography of quasiperiodic crystals *Acta Crystallogr.* A **52** 509–60
[14] Steurer W and Haibach T 1999 *Physical Properties of Quasicrystals* (*Springer Series in Solid State Sciences* vol 126) ed Z M Stadnik (Berlin: Springer) chapter 3, pp 51–90
[15] Steurer W and Haibach T 1999 The periodic average structure of particular quasicrystals *Acta Crystallogr.* A **55** 48–57